# Electrically Pumped Single-Mode Lasing Emission of Self-Assembled n-ZnO Microcrystalline Film/p-GaN Heterojunction Diode

**Zhen Guo, Dongxu Zhao,* Yichun Liu, Dezhen Shen, Bin Yao, Zhengzhong Zhang, and Binghui Li**

*Key Laboratory of Excited State Processes, Changchun Institute of Optics, Fine Mechanics and Physics, Chinese Academy of Sciences, Changchun 130021, People's Republic of China*

**Zhen Guo**

*Graduate School of the Chinese Academy of Sciences, Beijing 100049, People's Republic of China*

**Yichun Liu**

*Center for Advanced Optoelectronic Functional Material Research, Northeast Normal University, Changchun 130024, People's Republic of China*

*Received: June 1, 2010; Revised Manuscript Received: July 28, 2010*

The self-assembled ZnO microcrystalline film was synthesized through repeated growth by a low-temperature hydrothermal method using p-GaN wafer as a template. Well-defined peaks with 6-fold symmetry in the XRD $\phi$-scan indicated the repeated grown ZnO microcrystal following an orientation relationship of $[103]_{ZnO} \| [103]_{GaN}$. Room temperature photoluminescence (RT PL) spectra indicated that self-assembled ZnO owned a strong ultraviolet (UV) emission accompanied by a weak defects-related emission. The electrically pumped single-mode lasing emission located at 407 nm with a full width at half-maximum (fwhm) of 0.7 nm was observed based on the self-assembled n-ZnO microcrystalline film/p-GaN heterojunction diode.

## Introduction

ZnO is a promising material for the short-wavelength photonic applications due to its direct wide bandgap of 3.37 eV and the large exciton bounding energy of 60 meV,[1] which make it a potentially useful photonic material for ultraviolet (UV) lasers, photodetectors,[2−4] and other optoelectronic devices.[5−7] Optical pumped UV lasers have already been observed in ZnO thin films and ZnO nanostructures.[8,9] The cavity of the ZnO lasers could be formed by the end surfaces or the side surfaces of the hexagonal-shaped ZnO.[10−12] The well-regulated laser modes could be clearly observed.[8,10] Because of the high scattering in ZnO, random laser behavior could also be realized in ZnO nanostructures.[13] Compared with optical pumped stimulated emission of ZnO, electrically pumped ZnO laser was first realized on the ZnO/SiC heterojunction because of the lack of high-quality p-type ZnO.[13] After that, electrically pumped stimulated emissions were observed in different ZnO-based homojunctions and heterojunctions. In 2008, Sun et al.[14] reported a ZnO p−n homojunction nanorods laser diodes formed by As ion implantation. Random lasing from n-ZnO thin film/p-GaN heterojunction was also reported.[15] Although there were a few reports about the ZnO-based laser diodes, a single-mode laser has not been obtained.

Beside the emission line narrowing and the intensity nonlinear enhancement, the clear laser cavity mode is a definitive character for lasers. From the results reported by Tang[8] and Yang,[10] we could conclude the facets of the ZnO hexagonal structure could form the natural Fabry−Pérot (F−P) lasing cavities for the close-packed ZnO microcrystallite thin films or separated ZnO nanorods. To make an electrically pumped laser diode, the high reflected metal electrodes on the top of the ZnO may prevent the lasing emission from the top surfaces. Therefore, it is better to construct an edge emission laser diode based on ZnO. The essential for this approach is the formation of the laser cavity. Because it is difficult to naturally cleave the usually used sapphire substrate to form a cavity, we designed a self-assembled close-packed ZnO microcrystalline film to realize a naturally formed laser cavity.

In our work, the p-GaN wafer was used as a template to induce the growth of ZnO as well as holes injection layer. Ideal n-ZnO/p-GaN heterojunction could be built with self-assembled ZnO microcrystalline film by the hydrothermal method; most of the electrons are shown to be confined in ZnO while holes could be injected into the ZnO layer from p-GaN by band alignment of the n-ZnO/p-GaN heterojunction. In this way, an electrically pumped single-mode lasing emission located at 407 nm with fwhm of 0.7 nm was realized.

## Experimental Section

For the fabrication of n-ZnO/p-GaN heterojunction, undoped n-ZnO was fabricated onto commercially available p-GaN/sapphire substrate by a hydrothermal method using $Zn(CH_3COO)_2 \cdot 2H_2O$ and $C_6H_{12}N_4$ as reactant sources. The hole concentration and mobility were $3.0 \times 10^{17}$ $cm^{-3}$ and 10 $cm^2$ $V^{-1}$ $s^{-1}$, respectively, for p-GaN wafer. Prior to the growth the p-GaN/sapphire substrates were cleaned by organic solvents to remove contaminations. The p-GaN wafer was placed facing toward the bottom of the kettle during the growth in our case. The ZnO microcrystalline film was obtained through repeated growth for 6 times under the same conditions by the low-temperature hydrothermal method. The ZnO microcrystalline

* Corresponding author: e-mail dxzhao2000@yahoo.com.cn; Tel +86-431-86176322, Fax +86-431-86176298.

10.1021/jp105016b © 2010 American Chemical Society
Published on Web 08/23/2010

film could form epitaxially on the GaN layer because of the lower mismatch between them. In the hydrothermal growth process the reaction solution was adjusted to identical concentration for both sources (0.01 mol/L). The reaction kettle was put into an oven and maintained at 90 °C for 16 h for each experiment. The obtained samples were rinsed by deionized water. Bilayer Ni/Au and monolayer In electrodes were employed as the contacts for the p-GaN wafer and n-ZnO layers, respectively.

The morphology of the samples was investigated by the field-emission scanning electron microscopy (FESEM) using a Hitachi S4800 microscope. The crystal structure of the samples was studied by a Bruker D8GADDS X-ray diffractometer (XRD) using Cu Kα radiation with an area detector. PL measurement was performed using a JY-630 micro-Raman spectrometer with the 325 nm line of He−Cd laser as excitation source. The electrical characteristics of the diode were measured by a Lakeshore 7707 Hall measurement system. The EL spectra were performed by a Hitachi F4500 spectrometer, and a continuous-current power source was used to excite the diode. Note that all the measurements were performed at room temperature.

## Results and Discussion

The surface morphology of ZnO grown on p-GaN temple through 2 times, 4 times, and 6 times growth by the hydrothermal method are shown in Figure 1a−c, respectively. It is easy to observe that 2 times growth ZnO still displays hexagonal column morphology as shown in the inset of Figure 1a, and the formed ZnO merged each other after repeated growth. The connected web structures were obtained after 4 times growth shown in Figure 1b; the connected web structure can be divided into different size hexagonal columns. The inset of Figure 1b shows the typical combined interface of two hexagonal columns. The self-assembled ZnO microcrystalline film was formed after repeated growth for 6 times as shown in Figure 1c. The side surfaces of the most columns show natural combination morphology, and the top surface shows a smooth ZnO (0001) facet illustrating high crystalline quality shown in the inset of Figure 1c.

Figure 2a shows wide range (30°−70°) X-ray diffraction (XRD) 2$\theta$-scan of the ZnO microcrystalline film sample. As shown in the figure, only one diffractive peak located at 34.5° could be observed, which corresponds to the (002) direction of ZnO diffractive peak. This result indicates the ZnO microcrystalline film is the $c$-axis preferred orientation. Because the lattice parameters of ZnO and GaN are very close, a $\omega$-scan was performed to identify the ZnO (002) and GaN (002) diffractive peaks. From the inset of Figure 2a the (002) diffractive peaks originated from ZnO and GaN could be distinguished clearly with the corresponding narrow fwhm of 0.16° and 0.12°, which reveals the good crystal quality of ZnO microcrystalline film. The 2D-XRD image of the ZnO microcrystalline film is also shown in the inset of Figure 2a. The image of the film does not show any diffraction rings but gives a focused dot, which symbolizes the uniform in-plane atom alignment and the structural isotropy of the film. Figure 2b shows the in-plane-scan ($\phi$-scan) orientation relationship between ZnO microcrystalline film and the GaN wafer. The well-defined peaks showing a 6-fold symmetry are obtained, which is consistent with the wurtzite crystal structure. The respective peaks of ZnO and GaN are at the same angle on the $c$-axis, which results in ZnO and GaN have an in-plane orientation relationship of $[103]_{ZnO}\|[103]_{GaN}$. This result agrees well with the report from ZnO nanostructures on GaN by Kim et al.[16] The $\phi$-scan spectrum implies the same crystal facets from different ZnO microcrystalline film are parallel to each other without any rotations.

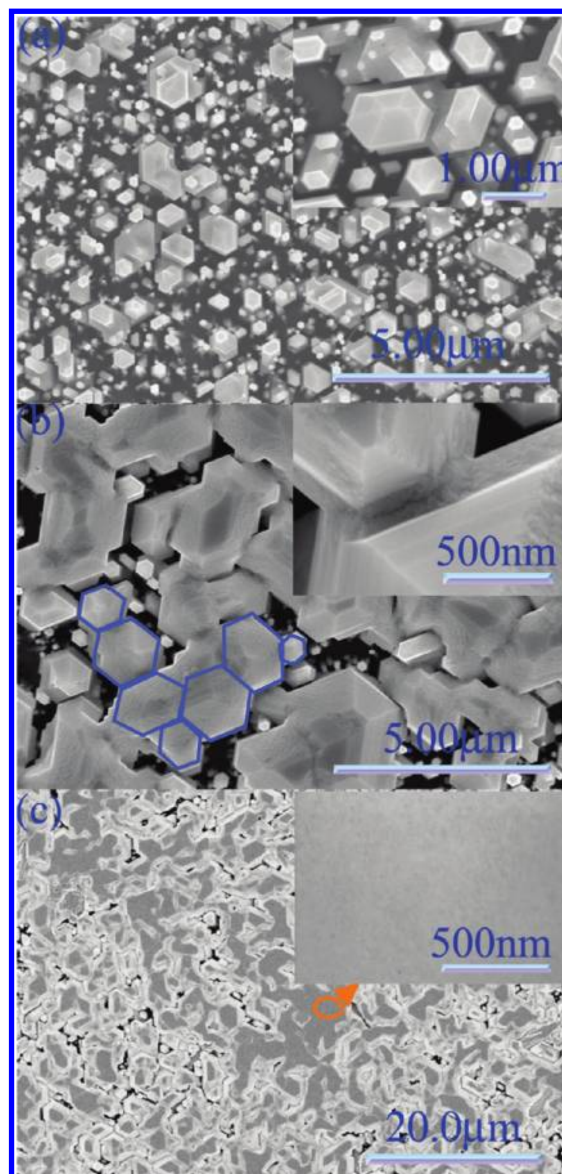


**Figure 1.** SEM images of ZnO samples grown on p-GaN wafer through 2 times (a), 4 times (b), and 6 times (c) by the hydrothermal method under the same conditions for each time growth. The insets of (a) and (b) show the magnified SEM images of 2 times and 4 times growth ZnO, respectively. The inset of (c) shows the top surface morphology as indicated by an arrow.

Figure 3 shows the RT PL spectra of ZnO layers through 2 times, 4 times, and 6 times growth by the hydrothermal method and p-GaN wafer. As shown in the figure, the spectra of all the ZnO samples display a dominant sharp near-band-edge (NBE) emission at about 380 nm accompanied by a weak deep-level emission at around 550 nm. It is also obvious to find out that 6 times growth ZnO microcrystalline film displays a dominant sharp near band-edge (NBE) emission at 377 nm while the UV peaks of the 2 times and 4 times growth ones are located at 383 nm, which may be due to the larger surface induced red shift. The PL spectrum of the p-GaN is dominated by a broad peak centered at about 420 nm, which is frequently observed in Mg-doped p-GaN corresponding to the transitions between conduction-band electrons or donors and Mg-related acceptors.[17] The fringes observed in the spectrum are due to the interference between GaN/air and the sapphire/GaN interfaces.

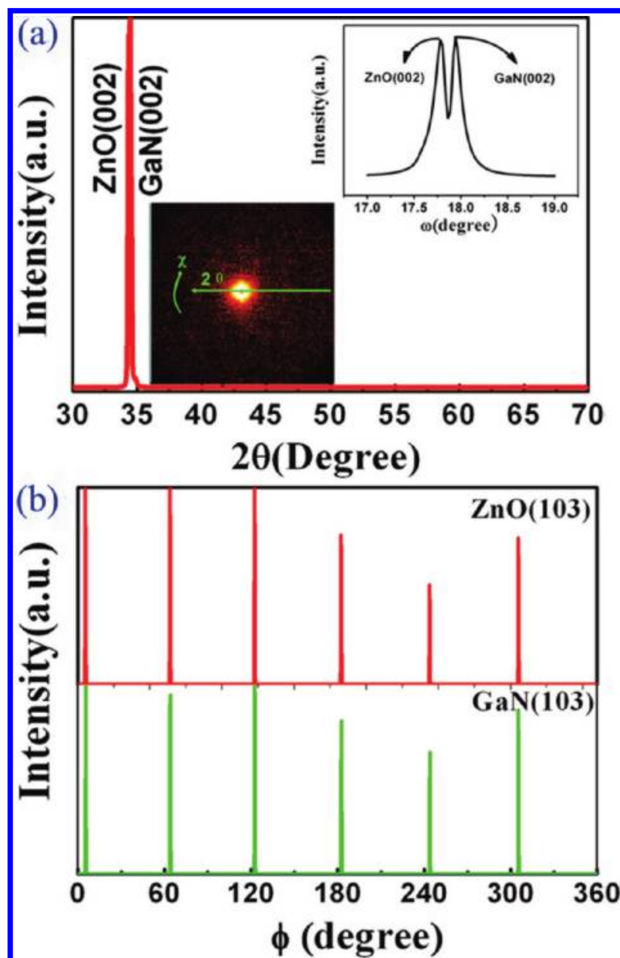


**Figure 2.** (a) Wide-range XRD $2\theta$-scan of the ZnO microcrystalline film grown on *p*-GaN/sapphire substrate. The upper trace of the inset shows XRD $\omega$-scan curve of the ZnO microcrystalline film (002) pattern. The lower trace shows the corresponding 2D XRD image of the ZnO microcrystalline film grown on GaN wafer. (b) XRD $\phi$-scans of the epitaxial ZnO microcrystalline film and GaN wafer.

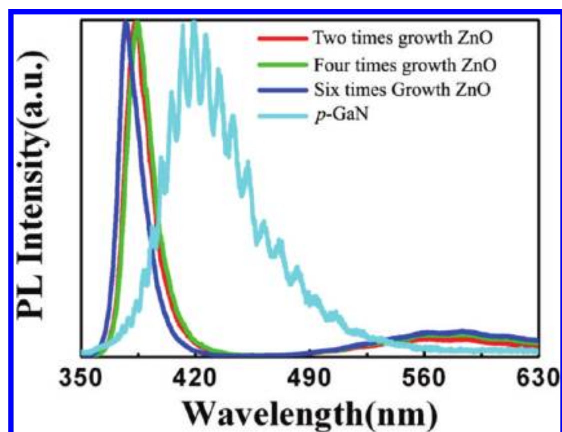


**Figure 3.** PL spectra of the ZnO samples and the p-GaN wafer.

To make a diode, Ni/Au and In electrodes were used for p-GaN wafer and n-ZnO microcrystalline film, respectively. The ZnO layer is comprised by the merged hexagonal columns as shown in the device scheme of Figure 4a. Figure 4b shows $I-V$ characteristic of a heterojunction device; a nonlinear rectifying behavior is observed. The linear curve for Ni/Au on p-GaN reveals that good Ohmic contacts have been obtained in the electrodes. As reported everywhere,[15,18] In metal can form good Ohmic contact to n-ZnO; from this point of view, we can

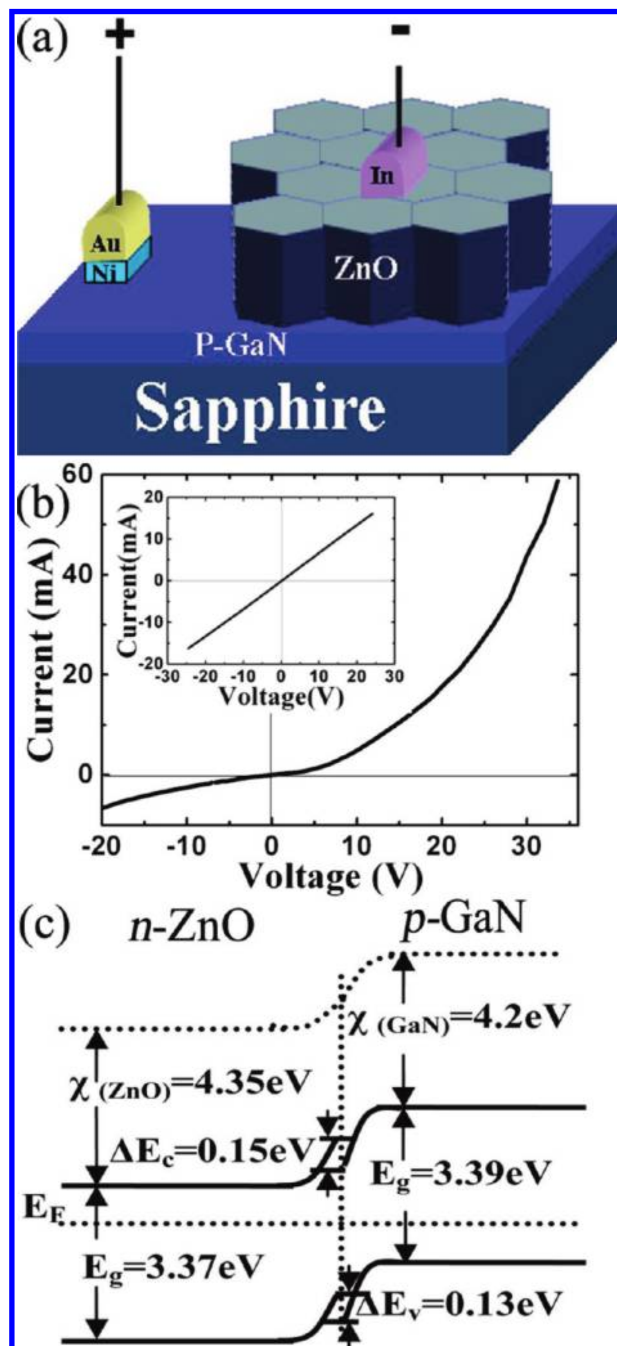


**Figure 4.** (a) Schematic diagram of the ZnO microcrystalline film/p-GaN heterojunction. (b) $I-V$ characteristic of the heterojunction showing a typical rectifying characteristic. The inset shows the $I-V$ characteristic of Ni/Au contacts to p-GaN wafer. (c) Energy band diagram of the n-ZnO/p-GaN heterojunction under zero bias.

conclude that the rectifying behavior of the LED originates from the n-ZnO microcrystalline film/p-GaN heterojunction. Figure 4c shows the ideal heterojunction band diagram for n-ZnO/p-GaN, which was constructed by following the Anderson model.[19] To construct the band diagram, the electron affinities ($\chi$) of ZnO and GaN were assumed to be 4.35 eV[20] and 4.2 eV,[21] respectively. The band-gap energies ($E_g$) are 3.37 and 3.39 eV for ZnO and GaN at room temperature. As shown in the energy band diagram, the energy barrier $\Delta E_C$ for an electron is $\Delta E_C = \chi_{(GaN)} - \chi_{(ZnO)} = 4.2 - 4.35 = -0.15$ eV, and the energy barrier $\Delta E_V$ for a hole is $\Delta E_V = E_g(\mathrm{GaN}) + \Delta E_C - E_g(\mathrm{ZnO}) = 3.39 - 0.15 - 3.37 = -0.13$ eV. There are two energy band offsets due to the different electron affinities and the band gaps between ZnO and GaN.

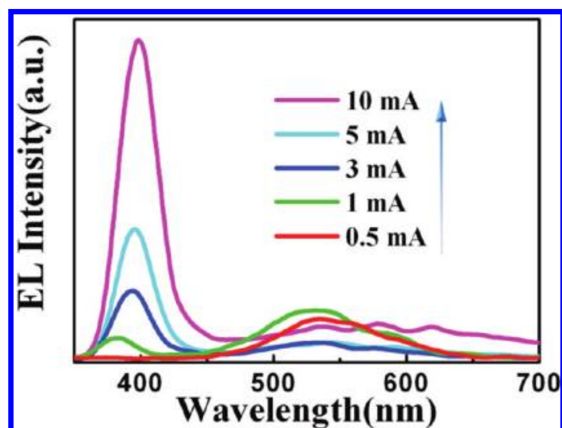


**Figure 5.** EL spectra of the n-ZnO microcrystalline film/p-GaN heterojunction under lower forward injection current.

By applying a forward bias onto the heterojunction, the EL spectra are collected from the edge of the device at room temperature. As shown in Figure 5, an emission peak centered at around 530 nm due to the interfacial recombination could be observed under lower driven current of 0.5 mA; a UV emission peak located at 383 nm appeared for a small portion of holes that are injected into n-ZnO from the p-GaN side with increasing the current to 1 mA. The UV emission peak becomes dominated and shifts to 392 nm accompanied by weak visible emission when the current further increased to 3 mA. A slight shift of peak position could also be observed with further increasing the injection current. This red shift is due to the band p emission under high injection current as often observed in optical pumped emission in ZnO. These results imply the recombination zone of EL emission is mainly in ZnO, and the dominated UV EL emission peak could be attributed to the band edge emission from ZnO under lower forward injection current.

With increasing the applied current to 36 mA, the emission peak red-shifts to the longer wavelength side, for the thermal effect can also induce this kind of phenomenon as reported by Yu et al.[22] And some very sharp peaks superimposed on a broad emission are observed shown in Figure 6a; these sharp emission peaks become more clearly with further increasing the driven current. At 46 mA a single-mode lasing emission peak centered at 407 nm with fwhm of 0.7 nm is detected. The dependence of the integrated emission intensity on the injection current is shown in the inset of Figure 6a, from which a threshold of 27 mA could be obtained. When the applied current exceeds this point, the emission intensity increases nonlinearly. The sharp emission peak with the narrow fwhm, the threshold, and the clear emission mode imply that the electrically pumped single mode lasing action has been realized in n-ZnO microcrystalline film/p-GaN heterojunction diode. Figure 6b shows the electroluminescence spectra detected from the edge and the top surface of the diode at an applied current of 46 mA. The spectrum recorded from the top surface shows only a weak and broad UV emission, while a lasing action could be observed from the edge, which indicates the laser cavity may be formed directionally parallel to the substrate.

To realize electrically driven lasing, the efficient carrier accumulation and the laser cavity are essentials.[23] Because of $\Delta E_V < \Delta E_C$, larger $\Delta E_C$ blocks the escape of the majority carriers (electrons) in ZnO; meanwhile, the majority carriers (holes) in GaN could be efficiently injected into ZnO under forward bias. The injected holes from GaN into ZnO could recombine radiatively with the electrons in ZnO microcrystalline film. The self-assembled ZnO microcrystalline film in our case owns excellent crystal quality, and ideal interface can be formed due to the ZnO was freely synthesized by the low-temperature hydrothermal method.

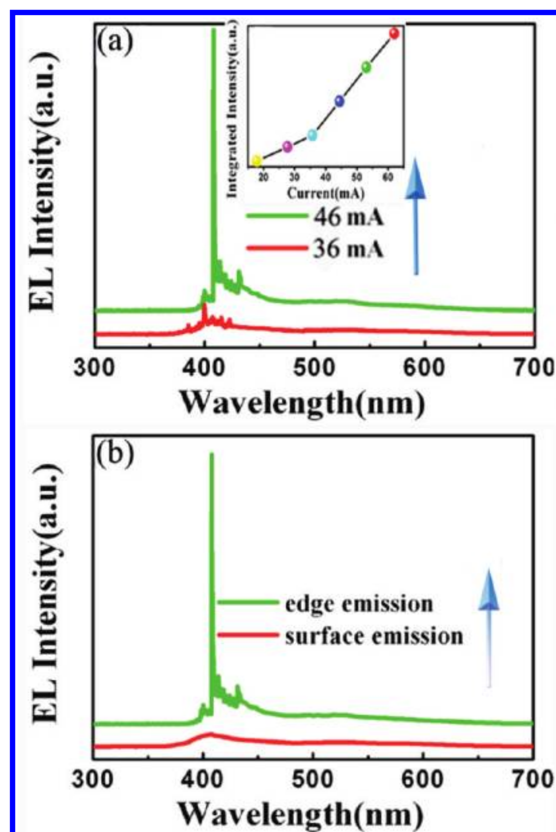


**Figure 6.** (a) Single mode lasing emission for the n-ZnO microcrystalline film/p-GaN heterojunction was obtained under higher forward injection current of 46 mA. The lasing effect is evident when the injection current exceeds 36 mA; the integrated EL intensity as a function of the injection current is shown in the inset. (b) The surface and the edge EL spectra of the diode under the same injection current of 46 mA.

Another key point to realize lasing action is the laser cavity formation. From the $\phi$-scan spectrum and SEM images it could be deduced same crystal facets from different ZnO microcrystalline film are parallel to each other without any rotations. Since the refractive index of ZnO (2.45) is larger than that of air (1.0), the parallel side-facets of the close packed ZnO microcrystalline film may serve as a mirror to form the laser cavities naturally.[24]

## Conclusion

In summary, the electrically pumped single-mode lasing emission operating at room temperature has been realized based on the self-assembled ZnO microcrystalline film fabricated on the p-GaN template. For the self-assembled ZnO could form an excellent interface with GaN wafer benefiting from the holes injection from GaN to ZnO; a single-mode lasing emission located at 407 nm with fwhm of 0.7 nm was observed. The reason for the red shift of the lasing emission peak may be due to the thermal effect; we believe that electrically pumped single-mode lasing emission located at the shorter wavelength for the self-assembled ZnO/p-GaN heterojunctions could be realized under optimal conditions.

**Acknowledgment.** This work was supported by the Key Project of National Natural Science Foundation of China under Grant No. 50532050, the "973" program under Grant Nos.

2006CB604906 and 2008CB317105, the Innovation Project of Chinese Academy of Sciences, and the National Natural Science Foundation of China under Grant Nos. 60506014, 10674133, and 60776011.

**Supporting Information Available:** Figure S. This material is available free of charge via the Internet at http://pubs.acs.org.

## References and Notes

(1) Liang, W. Y.; Yoffe, A. D. *Phys. Rev. Lett.* **1968**, *20*, 59.
(2) Kouklin, N. *Adv. Mater.* **2008**, *20*, 2190–2194.
(3) Park, W. I.; Jjun, Y. H.; Jung, S. W.; Yi, G. C. *Appl. Phys. Lett.* **2003**, *82*, 964.
(4) Law, L. B. K.; Thong, J. T. L. *Appl. Phys. Lett.* **2006**, *88*, 133114.
(5) Vayssieres, L.; Keis, K.; Hagfeldt, A.; Lindquist, S. E. *Chem. Mater.* **2001**, *13*, 4386.
(6) Johnson, J. C.; Yan, H. Q.; Yang, P.; Saykally, R. J. *J. Phys. Chem. B* **2003**, *107*, 8816.
(7) Fu, H. K.; Cheng, C. L.; Wang, C. H.; Lin, T. Y.; Chen, Y. F. *Adv. Funct. Mater.* **2009**, *19*, 3471–3475.
(8) Tang, Z. K.; Wong, G. K. L.; Yu, P. *Appl. Phys. Lett.* **1998**, *72*, 22.
(9) Zou, B.; Liu, R.; Wang, F.; Pan, A.; Cao, L.; Wang, Z. L. *J. Phys. Chem. B* **2006**, *110*, 12865–12873.
(10) Huang, M. H.; Mao, S.; Feick, H.; Yan, H.; Wu, Y.; Kind, H.; Weber, E.; Russo, R.; Yang, P. *Science* **2001**, *292*, 1897.
(11) Czekalla, C.; Sturm, C.; Grund, R. S.; Cao, B.; Lorenz, M.; Grundmann, M. *Appl. Phys. Lett.* **2008**, *92*, 241102.
(12) Wang, D.; Seo, H. W.; Tin, C. C.; Bozack, M. J.; Williams, J. R.; Park, M. *J. Appl. Phys.* **2006**, *99*, 093112.
(13) Leong, E. S. P.; Yu, S. F. *Adv. Mater.* **2006**, *18*, 1685.
(14) Yang, Y.; Sun, X. W.; Tay, B. K.; You, G. F.; Tan, S. T.; Teo, K. L. *Appl. Phys. Lett.* **2008**, *93*, 253107.
(15) Zhu, H.; Shan, C. X.; Yao, B.; Li, B. H.; Zhang, J. J.; Zhang, Z. Z.; Zhao, D. X.; Shen, D. Z.; Fan, X. W.; Lu, Y. M.; Tang, Z. K. *Adv. Mater.* **2009**, *21*, 1613–1617.
(16) Kim, J. H.; Kim, E. M.; Andeen, D.; Thomson, D.; DenBaars, S. P.; Lange, F. F. *Adv. Funct. Mater.* **2007**, *17*, 463.
(17) Nakamura, S.; Mukai, T.; Senoh, M. *Jpn. J. Appl. Phys.* **1991**, *Part 2, 30*, L1998.
(18) Jiao, S. J.; Zhang, Z. Z.; Lu, Y. M.; Shen, D. Z.; Yao, B.; Zhang, J. Y.; Li, B. H.; Zhao, D. X.; Fan, X. W.; Tang, Z. K. *Appl. Phys. Lett.* **2008**, *88*, 031911.
(19) Milnes, A. G.; Feucht, D. L. *Heterojunctions and Metal-Semiconductor Junctions*; Academic: New York, 1972.
(20) Aranovich, J. A.; Golmayo, D. G.; Fahrenbruch, A. L.; Bube, R. H. *J. Appl. Phys.* **1980**, *51*, 4260.
(21) Qiao, D.; Yu, L. S.; Lau, S. S.; Redwing, J. M.; Lin, J. Y.; Jiang, H. X. *J. Appl. Phys.* **2000**, *87*, 801.
(22) Li, H. D.; Yu, S. F.; Lau, S. P.; Leong, E. S. P.; Yang, H. Y.; Chen, T. P.; Abiyasa, A. P.; Ng, C. Y. *Adv. Mater.* **2006**, *18*, 771–774.
(23) Duan, X. F.; Huang, Y.; Agarwal, R.; Lieber, C. M. *Nature.* **2003**, *421*, 241.
(24) Kavokin, A. V.; Baumberg, J. J.; Malpuech, G.; Laussy, F. P. *Microvavities*; Oxford University Press: Oxford, 2007; p 13.

JP105016B